Journal of Engineering Science and Technology
Vol. 14, No. 2 (2019) 951 - 964

DEVELOPMENT OF A FLUORESCENCE DETECTION SYSTEM FOR HIGH-RESOLUTION MELTING ANALYSIS USING SILICON PHOTOMULTIPLIER

K. S. CHONG[1], N. A. DEVI[2], S. M. THEN[2], K. B. GAN[1,*]

[1]Centre for Advanced Electronics and Communication Engineering (PAKET), Faculty of Engineering & Built Environment, Universiti Kebangsaan Malaysia, 43600, UKM Bangi, Malaysia
[2]School of Biomedical Science Faculty of Medicine & Health Sciences, University of Nottingham Malaysia Campus, 43500, Semenyih, Selangor, Malaysia
*Corresponding Author: gankokbeng@ukm.edu.my

Abstract

The introduction of fluorescent dye in the Polymerase Chain Reaction (PCR) assay has overcome the limitation of post-PCR analysis. Real-time PCR instruments have been developed to excite the fluorescent dye and detect the fluorescence light emits from the fluorescent dye during PCR and High-Resolution Melt (HRM) reactions. However, the cost and the size of existing benchtop instruments have limited its application for near patient testing. In this paper, a fluorescence detection system was designed and developed for high resolution melting analysis. The system used Light Emitting Diodes (LEDs) and Silicon Photomultipliers (SiPMs) as an excitation light source and fluorescent detector, respectively. The developed system can detect the fluorescence signal during the PCR and HRM processes. The development cost and the size of the system are lower and smaller compared to the real-time PCR instruments in the market. The developed system has overcome the limitation of existing real-time PCR instruments and improve the clinical facilities in developing country, especially for near patient testing.

Keywords: Fluorescence detection, High-resolution melting, Polymerase chain reaction, Real-time PCR, Silicon photomultiplier.

1. Introduction

PCR was developed in the 1980s by Kary Mullis, who received the Nobel Prize in 1994 [1]. PCR is an in vitro method that enzymatically amplifies specific DNA sequences by using oligonucleotide primers that flank the region of interest in the target DNA [2]. Traditional methods of cloning a DNA sequence into a vector and replicating it in a living cell often required days or weeks of work, but it can be done in a few hours by using PCRs. PCR is a common method used in the molecular biology labs to amplify DNA fragments and detect DNA sequences within a cell or environment [3, 4]. However, it requires post-PCR analysis, such as gel electrophoresis and image analysis to analyse the amplified DNA sequence at the ends of the PCR reaction [2]. The post-PCR analysis is a labour-intensive and not easily automated or adapted for high-throughput application. Furthermore, Filion [5] explained that the process of the quantification of nucleic acids is arduous.

The introduction of fluorescent binding dye in the PCR assay has modified the conventional PCR technique into another method, which is called as real-time PCR. Real-time PCR has overcome the limitation of post-PCR analysis [5, 6]. It accurately quantifies the initial amounts of targeted DNA sample in the PCR assay. The fluorescent binding dye in the real-time PCR assay is a double-stranded DNA (dsDNA) binding dyes or dye molecules, which it attaches to the PCR primers, or probes that hybridize with the PCR product during amplification. The dye emits fluorescence light when it binds to the double-stranded DNA. Based on studies by Valasek and Repa [7], the intensity of fluorescent light is directly proportional to the number of PCR amplicons generated in the PCR process. The fluorescence light is collected during the exponential phase of the PCR process. Yang et al. [8] proposed that the real-time PCR has revolutionized the field of molecular diagnostics and the technique, which is being used in a rapidly expanding number of applications such as HRM. HRM is a post-PCR analysis, which is used to identify genetic variation in targeted DNA samples.

The real-time PCR instrument consists of three basic parts: a thermal cycler system to perform temperature cycling, an optical system to emit light necessary for the activation of the fluorophore combined with a system to capture the generated fluorescence and a software to control the instrument operation, collect and analyse the recorded fluorescence signal [8, 9]. The data quality and reproducibility of real-time PCR analysis are governed by the performance of the thermal cycler and optical systems. The precision of the thermal cycle system and the sensitivity of the optical detection system are critical for high-performance applications such as HRM curve analysis [10, 11]. The HRM melt curve analysis involves the amplification of the region of interest in DNA using standard PCR techniques and follows by dissociation of double-stranded DNA in the presence of fluorescent dye. The fluorescent dye is highly fluorescence when bound to double-stranded DNA and poorly fluorescence in the unbound state. Accordingly, to Erali et al. [12], the change in fluorescence allows the analysis of genetic mutation or variance in nucleic acid sequence. The selection of a sensor and an actuator for the thermal cycler and optical detection system can affect the performance of real-time PCR instruments.

There are many types of optical detection systems have been introduced in the real-time PCR instruments to improve optical sensitivity. There are two main components in the optical detection system, namely excitation light sources and the light detectors. The excitation light source is used to excite the fluorescence dye and

the light detector is used to capture the emitted fluorescence light from the fluorescence dye. Most of the real-time PCR instruments use light-emitting diodes (LEDs) as the excitation light source [13-17]. The main advantage of the LEDs light source is that it has a longer life span and the intensity can be maintained constantly throughout its lifetime. Some of the real-time PCR instruments use tungsten halogen and Xenon lamp as the light source [18-20]. Compared to the LEDs, the tungsten halogen and Xenon lamp's intensity decay over time and it needs to be replaced.

Besides that, the sensor used in the real-time PCR instruments is the fluorimeter [13], Photo-Multiplier Tubes (PMTs) [15], photodiodes [14, 16] and charge-coupled device (CCD) camera [17-20]. Most of the high-throughput real-time PCR instrument uses a CCD camera to detect the fluorescence signal from all wells simultaneously. However, this approach leads to a more complicated mechanical structure. Some of the instruments [14-16] utilize multiple photodiodes or PMTs to avoid complicated mechanical structure.

The emerging of semiconductor technology, the SiPMs has been introduced and become the next generation of light detector [21]. SiPMs is a new kind of semiconductor light-detector and it is promising for higher detection efficiency compared to PMTs [22, 23]. SiPMs is an avalanche photodiode array joined together on a silicon substrate. The array is composed of photodiode and quenching resistor microcells arranged in parallel. SiPMs have single-photon sensitivity because each individual microcell can detect an incident photon. When a photon is detected, the microcell avalanches as the silicon becomes conductive and amplifies the current (Geiger discharge process). The quenching resistors then stop the avalanches, and the microcells are reset to detect another photon. The released current from all of the microcells can be measured to detect the intensity of light [24, 25]. Therefore, the number of microcells activated is proportional to the amount of incident light. The advantages of SiPMs are high sensitivity, low operating voltage and high timing performance. Several works have been highlighted the advantages of SiPMs such as high sensitivity, low cost and small physical size compared to commercial traditional light detectors [26-28].

Until now, the SiPMs detector has not been reported in the literature for real-time PCR instruments. The CCD camera and PMT detector used as an optical detector system in real time PCR instruments increase the physical structure and its cost. It limits the real-time instrument in a laboratory setting and not possible for near patient testing. Normally, according to Santangelo et al. [29], laboratory test needs longer turnaround time and may not be suitable for patients who need immediate treatment. Furthermore, the cost of this instrument has limited its usage in less-developed countries due to limited laboratory infrastructure. The aim of this study is to design and develop a portable and cost-effective fluorescence detection system. It uses LEDs as the excitation light source and the SiPMs as the fluorescence detector. The proposed method addressed the limitation of the conventional real-time PCR instrument.

2. Methods

2.1. Fluorescence detections system design

The fluorescence detection system consists of a thermal cycler system, a fluorescence acquisition system, a multifunction data acquisition device, a personal

computer and a power management module. Figure 1 shows the block diagram of the fluorescence detection system. The thermal cycler system was used to amplify the HRM assay. The system rapidly heats and cools the HRM solution according to the PCR and HRM protocol. Chong et al. [30] explained that the thermal cycler system has been designed and verified in our study. The fluorescence acquisition system was designed to detect the fluorescence light during PCR and HRM processes. The system excited the reaction mixture using LED light sources and detected the fluorescence signal using SiPMs. The multifunction data acquisition device (USB-6003, National Instruments) was used to control the thermal cycler and the fluorescence acquisition system. It digitized the fluorescence signal from the fluorescence acquisition system and sent it to the personal computer for further processing. The fluorescence signal was analysed using MathWorks software (Matlab 2017a). The power management module was developed to convert the alternating current (AC) power supply into direct current (DC). It supplies power to the thermal cycler and the fluorescence acquisition system.

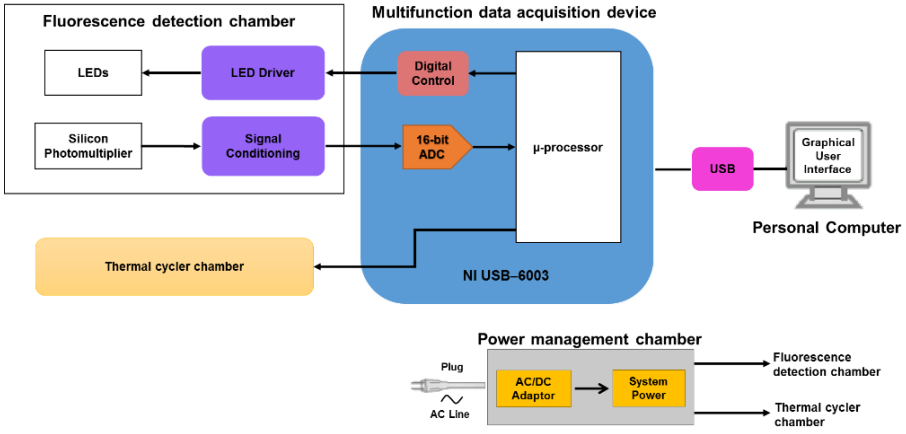

Fig. 1. Block diagram of fluorescence detection system.

2.2. Fluorescence optical path design

Figure 2 shows the fluorescence optical path design. The optical path was designed without involved in mechanical structure, especially lens that required precision. This can reduce the development cost and reduced the system complexity. The fluorescence detection system comprises six light detection channels to detect the fluorescence signal from the six PCR tubes. Each detection channel consisted of an excitation light source and an emission light detector. A high brightness Light-Emitting Diode (LED) with a glass lens (LED470L, Thorlabs) was used as the excitation light source for the fluorescence dye excitation. The LED470L has a peak spectral output at 470 nm. The LED470L is a compact, energy-efficient light source and emit light over a wide range of wavelengths compared to the Laser and Xeon lamp. The high-power consumption and heat generated from Laser and Xeon lamp have constrained the system development. It required an additional cooling system to cool down the Laser and Xeon lamp. Low noise and blue-sensitive SiPMs (MicroFC-10050-X18, SensL) with low-light detection capabilities were used to detect the fluorescence signal. The spectral range of the SiPMs is 300 to 800 nm and the maximum responsivity of the MicroFC-10050-X18 is 420 nm.

Two optical filters, namely an excitation filter and an emission filter were used in the fluorescence detection system. The excitation filter filters the unwanted wavelength and transmits the specific wavelengths of the LED470L to excite the fluorescence dye. The light emitted from the PCR tube contained the mixture of fluorescence light and the excitation light source as shown in Fig. 2. The emission filter filtered the light transmitted from the PCR tube to the detector (MicroFC-10050-X18).

The peak excitation and emission of fluorescence dye (EvaGreen) is 471 nm and 530 nm, respectively. Table 1 shows the specifications of the excitation and emission filters were used in this study. The filters were customized based on the EvaGreen specification. The central wavelength of the excitation filter was 470 nm with a full width at half maximum (FHWM) of 60 nm. The filter was placed between the PCR block and the LED470L. A customized plano-convex lens was used to collimate the fluorescence signal emitted from the PCR tube. This improved and increased the fluorescence signal before it detected by a detector. The plano-convex lens is a convergent lens with one convex surface and one flat surface. It focuses parallel light rays to a positive focal point. The plano-convex lens was placed in front of the PCR tube. The collimated fluorescence light from the lens was passed through the emission filter to a detector. The central wavelength of the emission filter was 523 nm with FWHM of 20 nm. The emission filter was placed between the plano-convex lens and the detector. Figure 3 shows the excitation and emission spectra of EvaGreen and the optical filters.

Table 1. Excitation and emission filter specification.

Property	Excitation filter	Emission filter
Material	CDGMH-K9L	CDGMH-K9L
Central wavelength (mm)	470	523
Full width at half maximum (FWHM) bandwidth (mm)	60	20
Dimension, length × width (mm)	26×6 ± 0.5	5.8 ± 0.5
Thickness (mm)	4 ± 0.5	4 ± 0.5

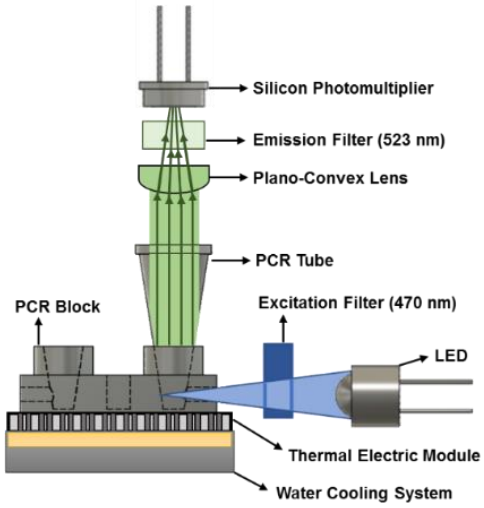

Fig. 2. Single channel optical filtering arrangement for fluorescence acquisition system.

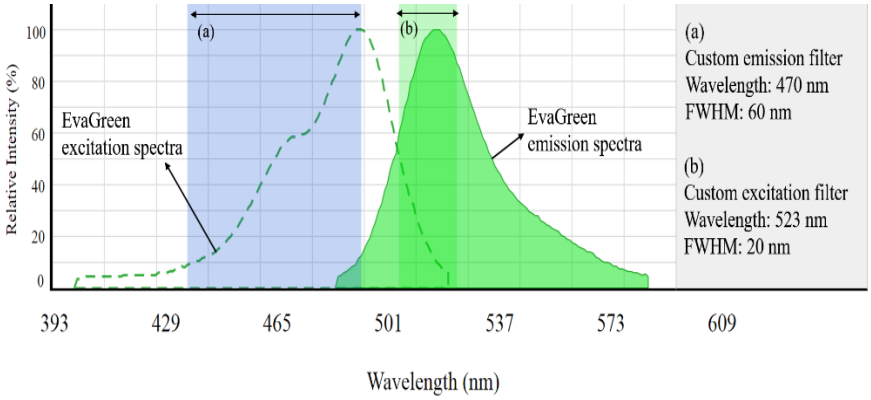

Fig. 3. Customized emission and excitation filters spectra.

2.3. Signal conditioning circuit

The six LED470L were connected in series to an LED driver circuit. The circuit was constructed by using a constant-current sink integrated circuit (CAT4101, On Semiconductor). The LED driver circuit was developed to provide a constant current source (0.33 A) to the six LEDs. The current source was determined by the resistance connected to the RSET pin. The LED driver circuit had a very low voltage dropout of 0.5 V at full load. The pin EN/PWM was connected to the digital control of NI USB-6003 for LED brightness adjustment and on-off switching.

Each SiPMs was connected to a transimpedance amplifier circuit. Figure 4 shows the transimpedance amplifier circuit using an ultra-low input bias current precision amplifier (LMP7721MA/NOPB, Texas Instruments). The transimpedance amplifier circuit amplified and converted the current from the detector into the voltage. The gain resistor and feedback capacitors on the circuit were 200 *kΩ* and 12 pF, respectively. The input bias current of the LMP7721MA/NOPB is 3 *fA*, with a specified limit of ±20 *fA* at 25 °C and ±900 *fA* at 85 °C. It has a low voltage noise (6.5 nV/√Hz), low DC-offset voltage (±150 µV maximum at 25 °C) and a low-offset voltage temperature coefficient (-1.5 µV/°C).

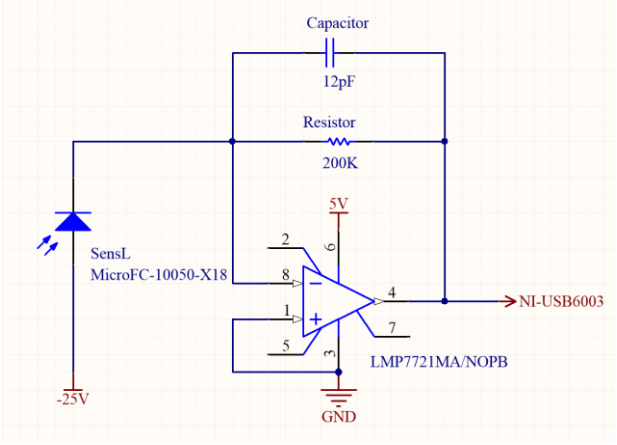

Fig. 4. Transimpedance amplifier circuit.

2.4. HRM solution preparation

The developed fluorescence detection system was evaluated by using an optimized 20 μL HRM assay. Optimization is required to ensure that the assay is sensitive and specific to the target of interest. HRM assay contained 10 μL of 2x SensiFast HRM mix (Bioline, USA), 0.8 μL of 0.4 uM of forward and reverse primers, 5 μL of RNAase-free water (Qiagen, Germany) and 500 ng of DNA template. SensiFast HRM contains EvaGreen fluorescence binding dye. The excitation and emission spectra of EvaGreen are 471 nm and 530 nm, respectively. EvaGreen has low fluorescence in the absence of double stranded DNA and high fluorescence in the presence of double-stranded DNA.

Table 2 shows the temperature and dwell time of the PCR and HRM reaction protocol. The PCR reaction started with an initial denaturation of 120 seconds at 95 °C, followed by 35 cycles of denaturation at 94 °C, annealing at 50 °C and extension at 72 °C. The period for each process were 60 seconds for denaturation, 20 seconds for annealing and 25 seconds for the extension. The PCR ended at the final extension process at 72 °C for 600 seconds.

At the end of the PCR process, there are three more steps for HRM thermal cycling processes. The temperatures of pre-melt, staring melting the end melting were 95 °C, 55 °C and 95 °C, respectively. The period for each HRM process was 30 seconds. The temperature resolution of HRM was 0.1 °C per seconds. The total time required to complete the whole protocol is 1 hour 28 minutes 5 seconds.

Table 2. PCR and HRM protocol which each process has specific heating temperature and dwell times.

Stage	Process	Temperature (°C)	Dwell time (s)	Number of cycles
PCR	**Initial denaturation**	95	120	1
	Denaturation	94	60	
	Annealing	50	20	35
	Extension	72	25	
	Final extension	72	600	1
HRM	**Pre-melt**	95	30	1
	Start melting	55	30	1
	End melting	95	30	1

3. Results and Discussion

The optical fluorescence detection system was successfully designed and developed as shown in Fig. 5(a). The top section of the system was the thermal cycling system and the fluorescence acquisition system. The signal conditioning circuit and multifunction data acquisition device were placed in the middle of the system.

The power management system was placed beside the system. The casing of the thermal cycling system was designed by using the Teflon plastic material. The Teflon plastic material has a high-temperature melting point (326.8 °C) which can hold the thermal cycling system (95 °C) and heating lid (120 °C). The heating lid was used to prevent the reaction mixture condensed around the PCR tubes.

Condensation of the reaction mixture will affect the PCR reaction and block the fluorescence signal being detected by the detector.

Figure 5(b) shows the developed fluorescence detection system. The DNA samples were excited independently at the left and right side of the block. The emitted fluorescence lights were collected separately at the top of the PCR tube. An optical baffle was placed in between the PCR tubes to prevent light interference.

The enclosure of the fluorescence acquisition system was designed using aluminium material. Two units of Peltier with a cooling fan were attached to the fluorescence detection enclosure. Figure 6 shows the relationship between the recorded fluorescence signal using SiPMs detector and the enclosure temperature. Initially, the enclosure was heated up by the heating lid and the cooling system was turned off.

The enclosure temperature was measured and recorded by Fluke t3000 FC Wireless K-Type Temperature Module. The cooling system was turned on when the enclosure temperature exceeded 40 °C. At the same time, the fluorescence emission was captured and recorded by the data acquisition device. As the temperature of the enclosure decreased, the acquired fluorescence signal increased.

The fluorescence signal reached the maximum when the enclosure temperature was 22 °C. The Peltier cools down the enclosure and maintaining the temperature at 22 °C. The result showed that the SiPMs is a heat sensitive sensor. Its performance dropped when the enclosure temperature increased.

(a) **(b)**

Fig. 5(a) Developed real-time fluorescence detection system, (b) Fluorescence detection chamber with a on top heating lid.

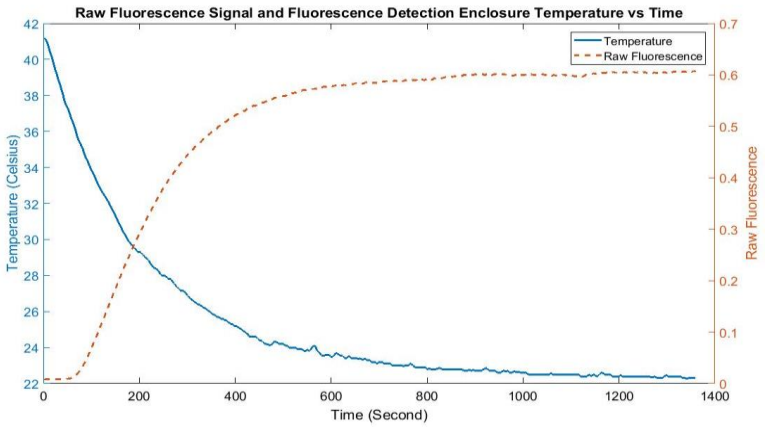

Fig. 6. Raw fluorescence signal and enclosure temperature versus time.

The developed fluorescence detection system was tested by the PCR and HRM processes. The HRM assay was heated up and cooled down by thermal cycler. The thermal cycler operates based on the PCR and HRM protocol as seen in Table 2. The fluorescence signal was captured during the PCR and HRM processes. The signal was analysed and plotted by using MathWorks software. Figure 7 shows the acquired fluorescence signal during the PCR reaction. As the PCR cycles increased, the amount of double-stranded DNA increased. More fluorescence binding dye attached to the double-stranded DNA strands. Hence, the fluorescence signal increased as the PCR cycles increased.

The signal was increased exponentially between PCR cycle 15 and 18. The cycle 15 to 18 was the exponential phase. In this phase, there was an abundance of the PCR reaction components and the PCR efficiency was equal to 100%. The fluorescence signal increased linearly between the PCR cycle 20 to 25. The cycle 20 to 25 was the linear phase. PCR efficiency slowly decreased after the exponential phase. This is because one or more components of the PCR reaction mixture reduced slowly below a critical concentration causing the PCR efficiency to decrease. After cycle 25, the PCR reached a plateau phase. The lack of PCR components such as deoxyribonucleotide triphosphates or primers caused a plateau phase of the PCR products. Therefore, the fluorescence signal did not increase.

Figure 8 shows the acquired fluorescence signals during HRM reaction. The fluorescence signals decreased as the temperature increased. During the HRM process, the amount of double-stranded DNA melted into single-stranded DNA increased as the temperature increased. The amount of fluorescence dye attached to the double-stranded DNA decreased and caused the fluorescence signal decreased. The rate of decreased fluorescence signal greater at the temperature around 83 °C to 89 °C. This is because the melting temperature (T_m) of the double-stranded DNA was around 87 °C. The rate of dissociation of double-stranded DNA into single-stranded DNA was increased when the temperature approach to the T_m.

The specification and cost of the developed fluorescence system were compared with the Eco (Illumina), CFX96 (Bio-Rad) and Rotorgene Q (Qiagen) real-time PCR system as shown in Table 3. The dimension of the prototype (22×15×40 cm)

was the smallest compared to the Eco (34×31×32 cm), CFX96 (33×46×36 cm) and Rotorgene Q (37×42×27 cm). The weight of the prototype (3.6 kg) was the lightest compared to the Eco (13.6 kg), CFX96 (21 kg) and Rotorgene Q (14 kg). The heating platform of the prototype, Eco and CFX96 were using Peltier while the Rotorgene Q was using air as its heating platform. The excitation light source of the Eco, CFX96, Rotorgene Q and the prototype are LED. The light detector of Eco, CFX96, Rotorgene Q and prototype are the CCD camera, photodiode, photomultiplier tube (PMT) and SiPMs, respectively. The number of emission filter channel of the prototype (1 Channel) was the lowest compared to Eco (4 channels), CFX96 (5 channels) and Rotorgene Q (6 channels). The prototype was designed to detect a specific fluorescence dye compared to the Eco, CFX96 and Rotorgene Q. Therefore, the cost of the developed prototype (MYR 22,285.00) was low compared to the Eco (MYR 114,338.44), CFX96 (MYR 172,173.00) and Rotorgene Q (MYR 166,942.00).

Table 3. Specification and cost of the commercial fluorescence detection system and the developed prototype [17, 31-33].

	Eco	CFX96	Rotorgene Q	Prototype
Dimension (cm) L×W×H	34×31×32	33×46×36	37×42×27	22×15×40
Weight (kg)	13.6	21	14	3.6
Heating platform	Peltier	Peltier	Centrifugal rotor with heated air	Peltier
Light source	Dual LED	6 LEDs	LEDs	6 LEDs
Excitation spectrum	2	5	2-6	440-500 nm
Detector	CCD camera	Photodiodes	PMT	SiPMs
Channels (emission filter, nm)	4 (505-545, 562-596, 604-644, 665-705)	5 (510-530, 560-580, 610-650, 675-690, 705-730)	2-6 (460, 510, 557, 610, 660, 712)	1 (510-530)
Instrument Cost (MYR)	114,338.44 (excluding shipping cost)	172,173.00	166,942.00	22,285.00

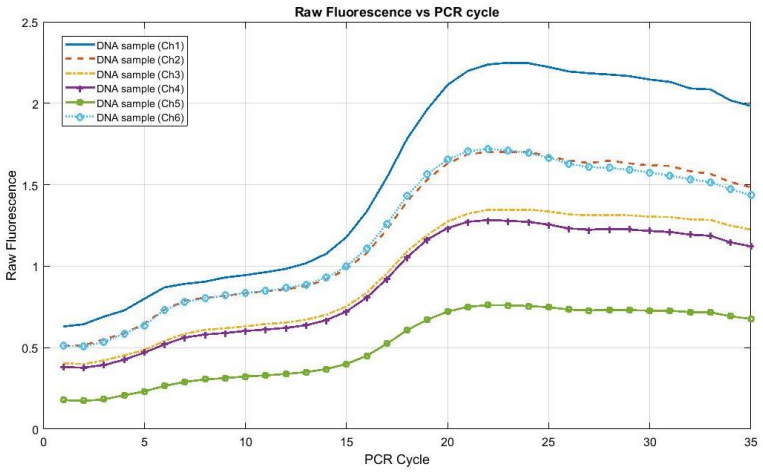

Fig. 7. Raw fluorescence signals versus PCR cycle.

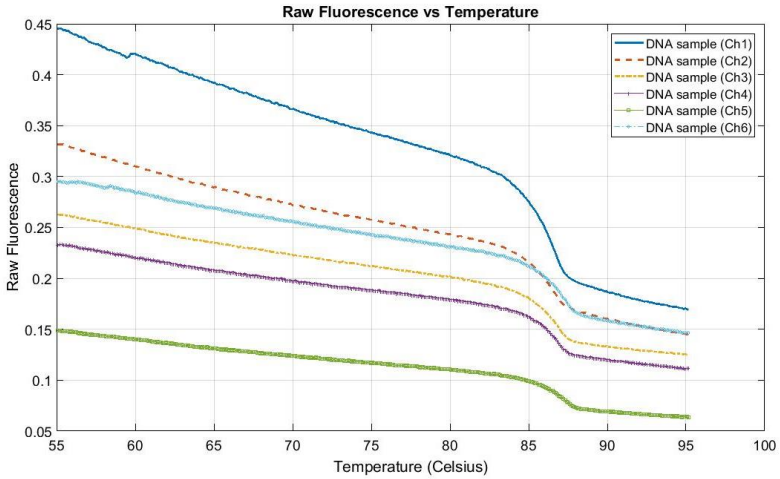

Fig. 8. Raw fluorescence signals versus temperature

4. Conclusions

A fluorescence detection system was successfully designed and built. It is lightweight and low cost compared to the available commercial systems. Our preliminary results showed that the SiPMs were heat sensitive detector. The SiPMs were maintained at 22 °C to obtain the maximum signal to noise ratio. The cooling system of the prototype can minimize thermal noise of the SiPMs. The system was able to capture the fluorescence signal during the PCR and HRM processes. One of the problems observed during the development of the system was that the amplitude of the fluorescence signals was not equal for each channel. As for future work, the fluorescence signal can be improved by using fluorescence signal normalization and temperature shifting algorithms to improve the fluorescence signal quality. Furthermore, a customized graphical user interface could be developed in the personal computer with a different melting curve analysis method. This device can be further extended into a genetic screening system for community health screening.

5. Acknowledgement

This research was supported by the Ministry of Higher Education (MOHE) of Malaysia under the Fundamental Research Grant Scheme FRGS/1/2016/TK04/UKM/02/5.

Nomenclatures

T_m	Melting Temperature, ºC

Abbreviations

AC	Alternating Current
CCD	Charge-Coupled Device
DC	Direct Current

DNA	Deoxyribonucleic Acid
dsDNA	Double-Stranded Deoxyribonucleic Acid
FHWM	Full Width at Half Maximum
HRM	High-Resolution Melting
LEDs	Light Emitting Diodes
MYR	Malaysian Ringgit
PCR	Polymerase Chain Reaction
PMTs	Photo-Multiplier Tubes
SiPMs	Silicon Photomultipliers

References

1. Alberts, B.; Johnson, A.; Lewis, J.; Raff, M.; Roberts K.; Walter, P. (2002). *Molecular biology of the cell* (4th ed.). New York: Garland Science.
2. Garibyan, L.; and Avashia, N. (2013). Research techniques made simple: Polymerase Chain Reaction (PCR). *The Journal of Investigative Dermatology*, 133(3), 8 pages.
3. Maheaswari, R.; Kshirsagar, J.T.; and Lavanya, N. (2016). Polymerase chain reaction: A molecular diagnostic tool in periodontology. *Journal of Indian Society of Periodontology*, 20(2), 128-135.
4. Valones, M.A.A.; Guimaraes, R.L.; Brandao, L.A.C.; de Souza, P.R.E.; Carvalho, A.d.A.D.; and Crovela, S. (2009). Principles and applications of polymerase chain reaction in medical diagnostic fields: A review. *Brazilian Journal of Microbiology*, 40(1), 1-11.
5. Filion, M. (2012). *Quantitative real-time PCR in applied microbiology*. Poole, United Kingdom: Caister Academic Press.
6. Arya, M.; Shergill, I.S.; Williamson, M.; Gommersall, L.; Arya, N.; Patel, H.R. (2005). Basic principles of real-time quantitative PCR. *Expert Review of Molecular Diagnostics*, 5(2), 209-219.
7. Valasek M.A.; and Repa, J.J. (2005). The power of real-time PCR. *Advances in Physiology Educationm*, 29(3), 151-159.
8. Yang, X.; Huo, F.; Yuan, H.; Zhang, B.; Xiao, D.; and Choi, M.M.F. (2011). Sensitivity enhancement of fluorescence detection in CE by coupling and conducting excitation light with tapered optical fiber. *Electrophoresis*, 32(2), 268-274.
9. Javorschi-Miller, S.; and Orlic, I.D. (2011*). Real-time PCR instrumentation: An instrument selection guide*. UK: Caister Academic Press.
10. Egholm, M.; Buchardt, O.; Nielsen, P.E.; and Berg, R.H. (1992). Peptide nucleic acids (PNA). Oligonucleotide analogs with an achiral peptide backbone. *Journal of the American Chemical Society*, 114(5), 1895-1897.
11. Gundry, C.N.; Vandersteen, J.G.; Reed, G.H.; Pryor, R.J.; Chen, J.; and Wittwer, C.T. (2003). Amplicon melting analysis with labeled primers: a closed-tube method for differentiating homozygotes and heterozygotes. *Clinical Chemistry*, 49(3), 396-406.
12. Erali, M.; Voelkerding, K.V.; and Wittwer C.T. (2008). High resolution melting applications for clinical laboratory medicine. *Experimental and Molecular Pathology*, 85(1), 50-58.

13. Herrmann, M.G.; Durtschi, J.D.; Bromley, L.K.; Wittwer, C.T.; and Voelkerding, K.V. (2006). Amplicon DNA melting analysis for mutation scanning and genotyping: cross-platform comparison of instruments and dye. *Clinical Chemistry*, 52(3), 494-503.
14. Idaho Technology Inc. (2018). LightScanner 32 System: Information sheet. Retrieved April 25, 2018, from https://www.bioke.com/blobs/Brochures/IT/LS32%20InfoSheet-0141.pdf.
15. ThermoFisher Scientific. (2018). StepOne and StepOnePlus Real-time PCR System. Retrieved April 25, 2018, from https://www.thermofisher.com/my/en/home/life-science/pcr/real-time-pcr/real-time-pcr-instruments/step-one-real-time-pcr-systems.html.
16. BioGene Ltd. - InSyte. (2018). WMD detector selector. Retrieved April 25, 2018, from https://www.wmddetectorselector.army.mil/detectorPages/151.aspx.
17. Roche Life Science. (2018). Roche molecular systems. Retrieved April 25, 2018, from https://lifescience.roche.com/en_my/products/lightcycler14301-20-instrument.html.
18. Illumina (2018). Eco real-time PCR system. Retrieved April 25, 2018, from https://support.illumina.com/real_time_pcr/eco_qpcr.html.
19. Applied Biosystems. (2018). Applied Biosystems 7300/7500/7500 Fast Real-Time PCR Systems. Retrieved April 25, 2018, from http://tools.thermofisher.com/content/sfs/manuals/cms_042676.pdf.
20. Fluidigm (2018). BioMark HD system. Retrieved April 25, 2018, from https://www.fluidigm.com/binaries/content/assets/fluidigm/biomark-hd-system.pdf.
21. Roche Life Science. (2018). LightCycler 480 Instrument II. Retrieved April 25, 2018, from https://lifescience.roche.com/en_my/products/lightcycler14301-480-instrument-ii.html.
22. Jackson, C.; Wall, L.; O'Neill, K.; McGarvey, B.; and Herbert, D. (2015). Ultra-low noise and exceptional uniformity of SensL C-series SiPM sensors. *Proceedings of the SPIE Optoelectronics, Photonic Materials and Devices Conference (OPTO).* San Francisco, California, United States. Volume 9359.
23. Grigoriev, E.; Akindinov, A.; Breitenmoser, M.; Buono, S.; Charbon, E.; Niclass, C.; Desforges, I.; and Rocca, R. (2007). Silicon photomultipliers and their bio-medical applications. *Nuclear Instruments and Methods in Physics Research Section A: Accelerators, Spectrometers, Detectors and Associated Equipment*, 571(1-2), 130-133.
24. Herbert, D.J.; Moehrs, S.; D'ascenzo, N.; Belcari, N.; Del. Guerra, A.; Morsani, F.; and Saveliev, V. (2007). The Silicon Photomultiplier for application to high-resolution Positron Emission Tomography. *Nuclear Instruments and Methods in Physics Research Section A: Accelerators, Spectrometers, Detectors and Associated Equipment*, 573(1-2), 84-87.
25. Guenther, B.; and Steel, D. (2004). *Encyclopedia of modern optics* (2nd ed.). Cambridge, Massachusetts, United States of America: Academic Press.
26. Dinu, N.; Amara, Z.; Bazin, C.; Chaumat, V.; Cheikali, C.; Guilhem, G.; Puill, V.; Sylvia, C.; and Vagnucci, J.F. (2009). Electro-optical characterization of SiPM: A comparative study. *Nuclear Instruments and Methods in Physics*

Research Section A: Accelerators, Spectrometers, Detectors and Associated Equipment, 610(1), 423-426.

27. Santangelo, M.F.; Pagano, R.; Lombardo, S.; Sciuto, E.L.; Sanfilippo, D.; Fallica; G., Sinatra, F., and Libertino, S. (2014). Silicon photomultipliers applications to biosensors. *Proceedings of the SPIE Optoelectronics, Photonic Materials and Devices Conference (OPTO).* San Francisco, California, United States. Volume 8990.
28. Mik, Ł.; Kucewicz, W.; Barszcz, J.; Sapor, M.; and Głąb, S. (2011). Silicon photomultiplier as fluorescence light detector. *Proceedings of the 18th International Conference on Mixed Design of Integrated Circuits and Systems (MIXDES).* Gliwice, Poland, 663-666.
29. Santangelo, M.F.; Sanfilippo, D.; Fallica, G.; Busacca, A.C.; Pagano, R.; Sciuto, E.L.; Lombardo, S.; and Libertino, S. (2014). SiPM as novel optical biosensor transduction and applications. *Proceedings of the Fotonica AEIT Italian Conference on Photonics Technologies.* Naples, Italy, 1-4.
30. Chong, K.S.; Gan, K.B.; and Then, S.M. (2017). Development of thermal cycler using proportional-integral controller for polymerase chain reaction. *Proceeding of the International Medical Device and Technology Conference (iMEDiTEC).* Skudai, Johor, Malaysia, 199-202.
31. Hawkins, R.C. (2007). Laboratory turnaround time. *Clinical Biochemist Reviews*, 28(4), 179-194.
32. Qiagen. (2018). Roto-Gene Q. Product specification. Retrieved April 25, 2018, from https://www.qiagen.com/us/shop/automated-solutions/pcr-instruments/rotor-gene-q/#technicalspecification.
33. Bio-Rad. (2018). CFX96 Touch Real-Time PCR Detection System. Retrieved April 25, 2018, from http://www.bio-rad.com/en-us/product/cfx96-touch-real-time-pcr-detection-system?ID=LJB1YU15.